Supporting information

Microchannel Plates to Screen Wall-coated Biocatalytic Flow Microreactors for Transamination Reactions

Nicolette Czarnievicz[a,b], Elwin Vrouwe[b] , Cecilia Córdoba-Quintero[a], Maciej Skolimowski[b] and

Fernando López-Gallego[a,c]*

[a] Center for Cooperative Research in Biomaterials (CIC biomaGUNE) - Basque Research and Technology Alliance (BRTA) Paseo de Miramón, 182, 20014 Donostia-San Sebastián, Spain.

[b] Micronit BV, Colosseum 15, 7521 PV Enschede, The Netherlands

[c] Ikerbasque, Basque Foundation for Science, Plaza Euskadi 5, 48009 Bilbao, Spain.

SUPPLEMENTARY METHODOLOGY

Design and microreactor fabrication

Given the desire to control the versatility of the design for diverse screening tests, the incorporation of flow functionality emerged as an attractive proposal. To include this capability, a connector part carefully filled with PDMS gaskets was added, which facilitated the inclusion of tubing (**Figure S1**).

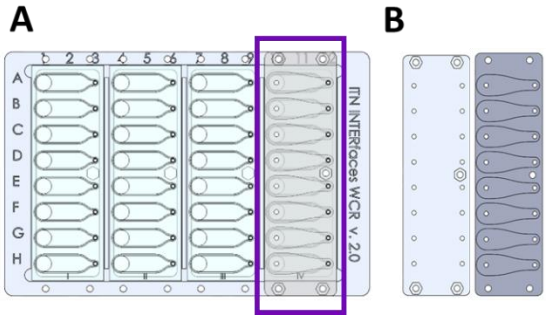

Figure S1. The design of the wall-coated microreactor plate includes the option to add flow capabilities. (A) Layout of the wall-coated microreactor plate, including screw holes in the frame for the tubbing connector attachment (in grey) highlighted in purple, and (B) tubbing connector attachment design (front (left image) and back (right image)). At the back can be observed the PDMS pockets (with the shape of the wide (inlet) and narrow (outlet) wells used as sealers for the system.

Calculation of microchannel volume and estimated maximum loading capacity of ATAs

The obtained design has a microchannel inner area of 296.36 $mm^{2,}$ calculated in the design program, SolidWorks®. This area was used to calculate the theoretical amount of enzyme fitting in each channel. For these calculations, the enzyme density used was reported by Fischer *et al*.[31] and is 1.35 g cm^{-3}. Using SEq1, the enzyme volume was determined where MW represents the molecular weight of the protein and ρ the protein density.

$$V_p\ (mm^3\ mol^{-1}) = \frac{MW(g\ mol^{-1})}{\rho(g\ cm^{-3})} x1000 \qquad \text{(SEq1)}$$

Using Avogadro's number ($6.022x10^{23}$ molecules mol^{-1}) and the volume, we determined the volume of one molecule using SEq2

$$V_m\ (mm^3\ molecule^{-1}) = \frac{V_p\ (mm^3\ mol^{-1})}{6.022x10^{\ 23}(molecules\ mol^{-1})} \qquad \text{(SEq2)}$$

Considering the volume of the protein as a cube, the length of each side was calculated to finally obtain the area of the protein. Then, dividing the inner surface of the microchannel through the protein area, the number of molecules that fit in the channel was deduced.

Applying Avogadro's number, the number of molecules can be converted to mol. Finally, using Avogadro's number, the mg of enzyme that fit in the microchannel was reached. As CvATA and HeATA are both dimeric enzymes, the calculation is the same in both cases, while PfATA is a tetrameric enzyme.

Epoxy-IDA-metal chelates surface functionalisation- verification.

An empty slide with each step of the functionalisation process was prepared. All the steps were also tested in an untreated microchannel as a negative control. To verify the activation step, RhBITC was added to an activated well; for the epoxide and, later, the IDA functionalisation, a fluorescent molecule ATTO550 that binds to the epoxide rings was used, and for the metal chelate functionalisation, an autofluorescent protein (m-Cherry) with a histidine tag was used. The different solutions were incubated for 1 hour, then rinsed with distilled water, and finally, the samples were visualised in the confocal microscopy ($\boldsymbol{\lambda}_{ex}$ 561 nm, objective 10X).

HMFA amination Setup

To follow the HMFA amination, an epoxy-IDA-Co^{2+} slide with His-PfATA immobilised on it, was flushed with a flow rate of 100 µL min^{-1} with the reaction mixture containing 10 mM HMF, 20 mM L-Alanine, 0.1 mM PLP in 25 mM HEPES, pH 8. All the microchannels were connected to recirculate the media through all of them.

.

WCµRs functionalisation with Epoxy-IDA-metal chelates

This functionalisation process entails a sequence of organised steps as depicted in **Figure S2**. The beginning involves the activation of the microreactor surface (PMMA) through the introduction of reactive amine groups, drawing inspiration from the method elucidated by Fixe *et al*.[30] Subsequently, the functionalisation aligned with the protocol defined by Pessela *et al* **(Figure S2**).[34] This sequential protocol consisted of the introduction of biepoxides, allowing them to attach to the pre-activated reactive amines on the surface. After this step, iminodiacetic acid was employed to open the remaining epoxide rings and to display dicarboxylic groups on the surface of the microreactor. This planned transformation prepares the microreactor's surface for the final step, the incubation with metal salts. This last step ends in the formation of distinct metal chelates on the surface of the PMMA wall-coated microreactor.

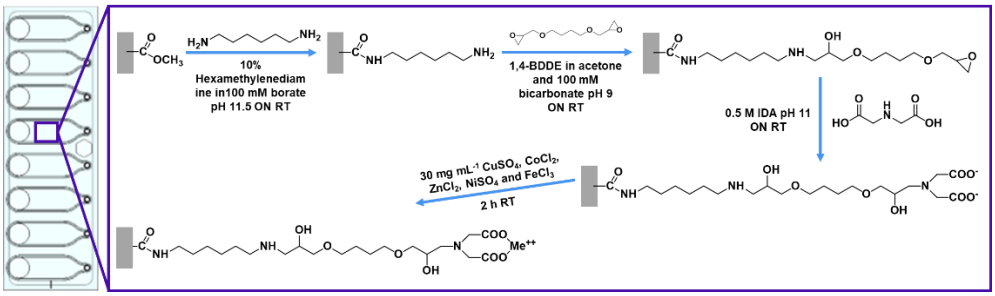

Figure S2. PMMA activation and surface functionalisation strategies. At the top, the surface activation and surface functionalisation with epoxide-IDA-metal chelate.

SUPPLEMENTARY RESULTS

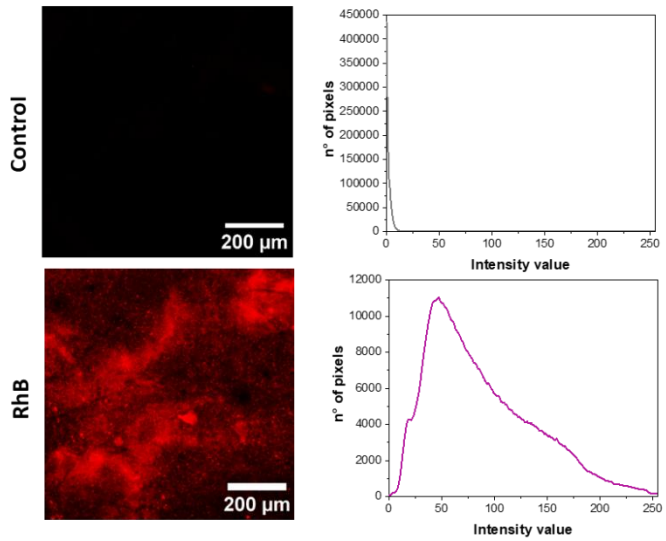

Figure S3. Analysis of PMMA activation using rhodamine B isothiocyanate (RhBITC). The control and the sample are presented as red fluorescent channels (left) and a histogram of fluorescent intensity per number of pixels in the picture (right). In all the cases, red fluorescence (λ_{ex} = 531 nm/λ_{em} = 593/40 nm) was used with a magnification of 10x.

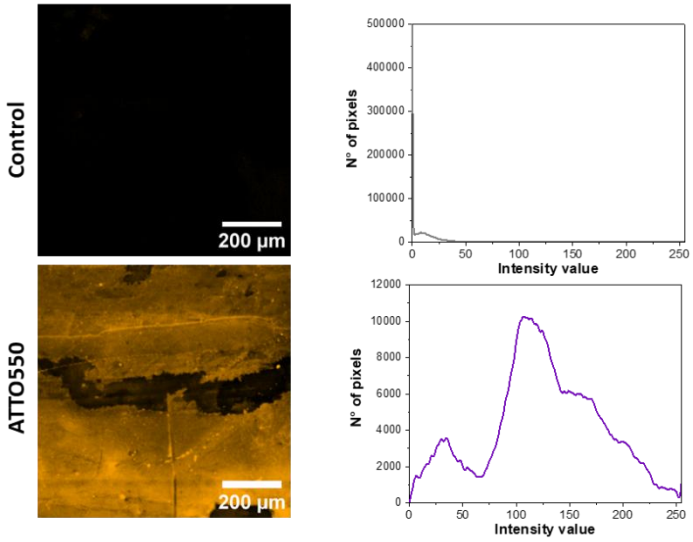

Figure S4. Analysis of the functionalisation with epoxides using aminated ATTO550. The control and the sample are presented as red fluorescent channels (left) and a histogram of fluorescent intensity per number of pixels in the picture (right). In all the cases, red fluorescence (λ_{ex} = 531 nm/λ_{em} = 593/40 nm) was used with a magnification of 10x.

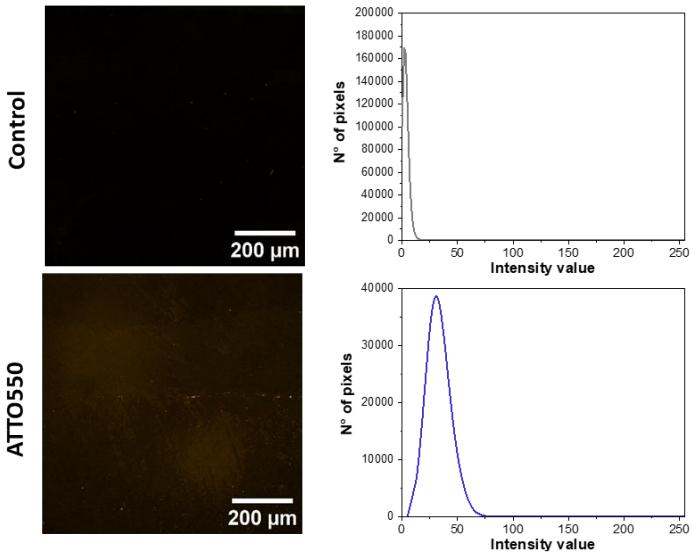

Figure S5. Analysis of the functionalisation with IDA using aminated ATO550. The control and the sample are presented in red fluorescent channels (left) and a histogram of fluorescent intensity per number of pixels in the picture (right). In all the cases, red fluorescence (λ_{ex} = 531 nm/λ_{em} = 593/40 nm) was used with a magnification of 10x.

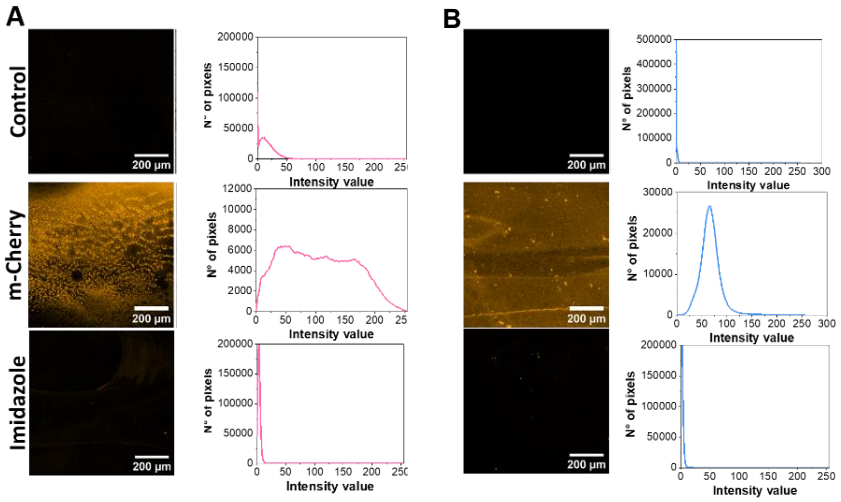

Figure S6. Analysis of metal chelates functionalisation through immobilisation of His-tagged red fluorescence protein (m-Cherry). (A) Functionalisation with Zn^{2+} and (B) with Cu^{2+}. Red fluorescence (λ_{ex} = 531 nm/λ_{em} = 593/40 nm) (right), and histograms of red fluorescence image (left) are presented for microreactors without m-Cherry (control), with m-Cherry (m-Cherry), and with m-Cherry eluted with 1 M imidazole (Imidazole). For all images, a magnification of 10x was used.

Table S1. GFP negative control. The GFP protein was incubated within the microchannels functionalised with iron-chelates for 15 minutes.

GFP	RFU	% GFP immobilised
Crude extract	4248637	-
Supernatant Epoxy-Fe slide	4177822	1

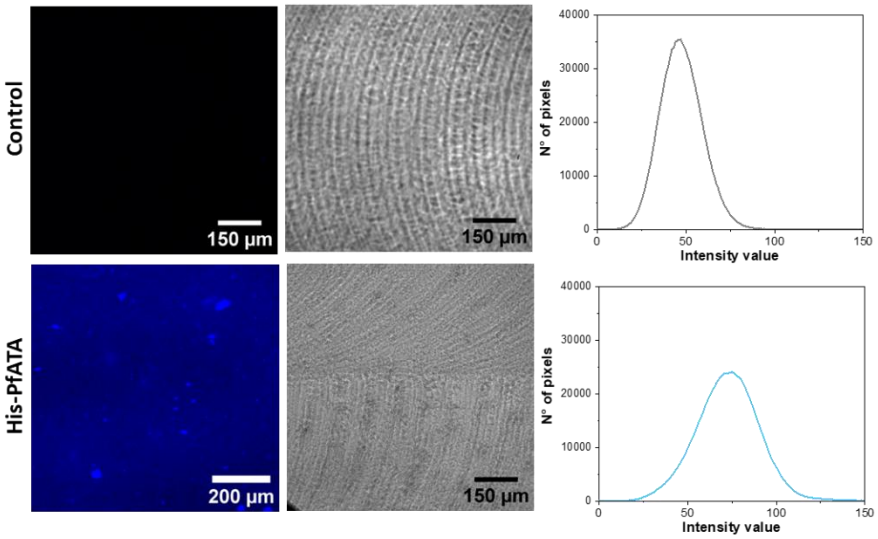

Figure S7. Transamination reaction in a microchannel. The control and the sample are presented as blue channels (left), brightfield channel (middle), and as a histogram of fluorescent intensity per number of pixels in the picture (right). The His-PfATA was immobilised in a microchannel functionalised with epoxy-IDA-Cu^{2+}. In all cases, a DAPI filter (λ_{ex} = 365 nm/λ_{em} = 447/90) was used and a magnification of 10x.

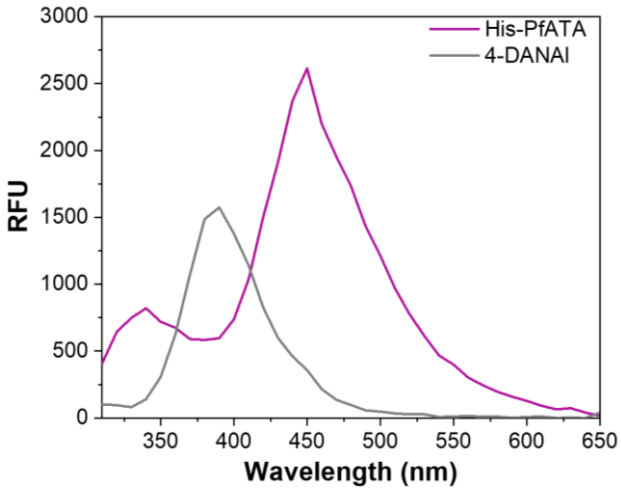

Figure S8. Fluorescent spectral scanning of a microreactor with His-PfATA immobilised in epoxy-IDA-Co^{2+}. In grey is depicted the spectrum for the mixture of reactions, manifesting the fluorescence from the 4-DANAl.

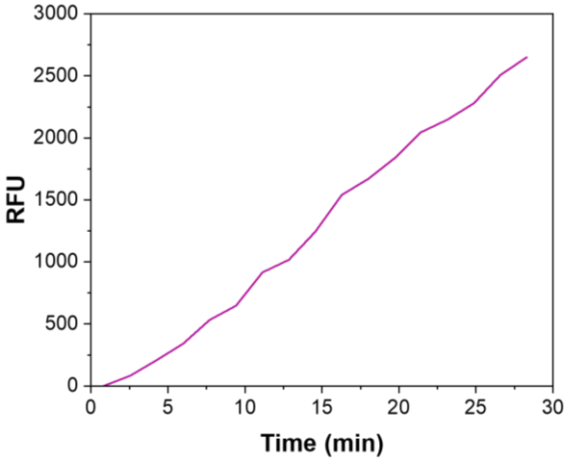

Figure S9. Time course of His-PfATA immobilised in an epoxy-IDA-Co^{2+} microreactor. The fluorescence was measured using an excitation wavelength of 290 nm and an emission one of 450 nm.

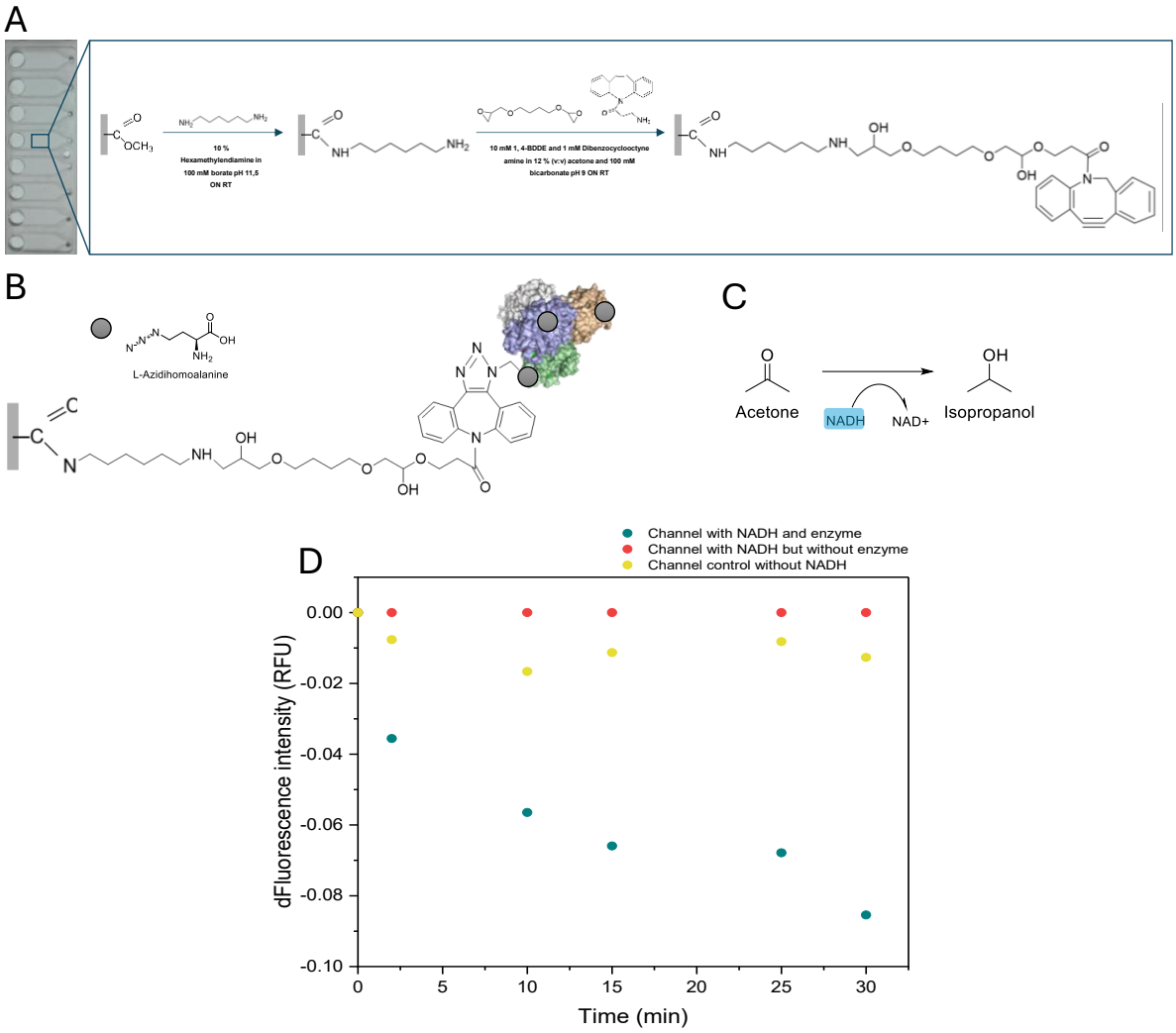

Figure S10. Immobilisation of alcohol dehydrogenase from Bacillus stearothermophilus (BsADH) bearing azidohomoalanine (AHA) on microreactors functionalised with cyclooctyne groups. (A) Synthetic route to functionalise the surface of PMMA microreactors with cyclooctyne groups. (B) Conjugation chemistry between BsADH with AHA and the microreactors with cyclootyne. (C) Enzymatic reaction catalyzed by BsADH and monitored by changes in the autofluorescence of NADH upon its oxidation. (D) Time course of NADH oxidation following the differences in fluorescence within the microreactor due to the action of BsADH immobilised on the microreactor walls. Blue dots: reaction with NADH and the enzyme. Red dots: reaction with NADH but without the enzyme. Yellow dots: reaction with the enzyme but without NADH.

Table S2. The maximum enzyme loading that can be immobilised on the inner surface of one microreactor. The inner surface area of the microchannel was 296.36 mm².

Enzyme	mol channel^{-1}	ng enzyme channel^{-1}
PfATA	1.25 x10^{-11}	2500
HeATA/CvATA	1.99x10^{-11}	2000

Table S3. Score determination raw data. After enzyme immobilisation (Column 1), microchannels were filled with the reaction mixture using 4-DANAl and incubated for 30 minutes to finally read in a fluorometer to determine total enzyme activity per microchannel (Column 2). After the initial evaluation, WCμRs underwent organic solvent incubation (30% DMSO, 16 hours). The solvent was removed, and transaminase activity was reevaluated (Column 3). Based on activity (U μchannel^{-1}) before (iA) and after (iA^{DMsO}) solvent incubation, we defined a score for ATA/metal-chelate pairs (Column 4).

Enzyme/Metal chelate	U/μchannel iA	U/μchannel iA^{DMSO}	Score = iA + 2x$iA^{(DMSO)}$
His-PfATA/Co^{2+}	15±4	8±4	30
His-PfATA/Cu^{2+}	12±0	0±0	12
His-PfATA/Fe^{3+}	16±13	0±0	16
His-PfATA/Ni^{2+}	24±41	0±0	24
His-PfATA/Zn^{2+}	21±3	1±1	22
PfATA-H3A/Co^{2+}	16±11	0±0	16
PfATA-H3A/Cu^{2+}	11±7	12±6	36
PfATA-H3A/Fe^{3+}	1±2	0±0	1
PfATA-H3A/Ni^{2+}	24±22	0±0	24
PfATA-H3A/Zn^{2+}	7±3	0±0	7
His-CvATA/Co^{2+}	15±0	0±0	15
His-CvATA/Cu^{2+}	19±31	0±0	19
His-CvATA/Fe^{3+}	11±17	0±0	11
His-CvATA/Ni^{2+}	28±41	0±0	28
His-CvATA/Zn^{2+}	8±12	0±0	8
CvATA-H2A/Co^{2+}	23±0	0±0	23
CvATA-H2A/Cu^{2+}	39±0	0±0	39
CvATA-H2A/Fe^{3+}	16±26	0±0	16
CvATA-H2A/Ni^{2+}	10±17	0±0	10
CvATA-H2A/Zn^{2+}	8±10	0±0	8
His-HeATA/Co^{2+}	16±5	0±0	16
His-HeATA/Cu^{2+}	13±10	0±0	13
His-HeATA/Fe^{3+}	1±1	0±0	1
His-HeATA/Ni^{2+}	18±10	7±5	33
His-HeATA/Zn^{2+}	14±12	0±0	14
HeATA-H4/Co^{2+}	19±2	0±0	19
HeATA-H4/Cu^{2+}	39±28	0±0	39
HeATA-H4/Fe^{3+}	20±9	0±0	20
HeATA-H4/Ni^{2+}	25±9	0±0	25
HeATA-H4/Zn^{2+}	28±23	0±0	28

SUPPORTING REFERENCES

31. F. Fixe, M. Dufva, P. Telleman and C. B. V. Christensen, *Nucleic Acids Res.*, 2004, **32**, e9-e9.
34. B. C. C. Pessela, C. Mateo, A. V. Carrascosa, A. Vian, J. L. García, G. Rivas, C. Alfonso, J. M. Guisan and R. Fernández-Lafuente, *Biomacromolecules*, 2003, **4**, 107-113